Inorg. Chem. **1989**, *28*, 2528-2533

Contribution from the Department of Chemistry, University of Houston, Houston, Texas 77204-5641,
and Laboratoire de Synthèse et d'Electrosynthèse Organométallique, Associé au CNRS (UA 33),
Faculté des Sciences "Gabriel", Université de Dijon, 21100 Dijon, France

Electrochemical and Spectral Characterization of Copper, Zinc, and Vanadyl *meso*-Tetrakis(1-methylpyridinium-4-yl)porphyrin Complexes in Dimethylformamide

K. M. Kadish,*[,1a] C. Araullo,[1a] G. B. Maiya,[1a] D. Sazou,[1a] J.-M. Barbe,[1b] and R. Guilard*[,1b]

Received August 3, 1988

The electrochemical and spectral characterization of copper, zinc, and vanadyl *meso*-tetrakis(1-methylpyridinium-4-yl)porphyrin complexes were investigated in dimethylformamide containing 0.1 M tetrabutylammonium perchlorate. Dc polarography, cyclic voltammetry, controlled-potential electrolysis, spectroelectrochemistry, ESR spectroscopy, and variable-temperature electrochemistry were used to characterize the electrode reactions and the products of each electroreduction. [(TMpyP)Cu]$^{4+}$, [(TMpyP)Zn]$^{4+}$, and [(TMpyP)VO]$^{4+}$ (where TMpyP is the porphyrin dianion) were reversibly reduced by six electrons in three well-defined two-electron-transfer steps, which occur between −0.50 and −1.20 V vs SCE. Two electrons were added to the porphyrin π ring system while an additional four electrons were involved in the reduction of the four *N*-methylpyridiniumyl substituent groups of [(TMpyP)M]$^{2+}$. An overall mechanism for the six-electron reductions of [(TMpyP)Cu]$^{4+}$, [(TMpyP)Zn]$^{4+}$, and [(TMpyP)VO]$^{4+}$ is proposed.

Introduction

meso-Tetrakis(1-methylpyridinium-4-yl)porphyrin complexes have been studied with respect to their importance in photochemical water splitting[2,3] and their interactions with nucleic acids and DNA.[4-8] The chemical and physico-chemical characterization of free base [(TMpyP)H$_2$]$^{4+}$ (where TMpyP is the porphyrin dianion) and eleven different metalated TMpyP derivatives have been reported in aqueous media.[9-17] Kano et al.[9,10] and Brookfield et al.[11] independently presented evidence for the stacking of free base [(TMpyP)H$_2$]$^{4+}$ in water, but Pasternack et al.[12,13] and Hambright et al.[14] reported that [(TMpyP)H$_2$]$^{4+}$ and [(TMpyP)VO]$^{4+}$ were monomeric in aqueous media. [(TMpyP)Ni]$^{4+}$ is also monomeric in aqueous media over the pH range 2–9,[12,13] as is [(TMpyP)VO]$^{4+}$.[13] However, this is not the case for these two TMpyP complexes in alkaline aqueous solutions where a dimerization has been shown to occur.[15] It has also been suggested that the anion radicals which are generated by the one-electron chemical reduction of [(TMpyP)H$_2$]$^{4+}$, [(TMpyP)M]$^{5+}$, where M = Al(III) or Ga(III), and [(TMpyP)M]$^{4+}$, where M = Zn(II) or Pb(II), probably dimerize in aqueous media and that these dimers disproportionate to give a neutral porphyrin complex and a phlorin.[16,17]

The *N*-methylpyridiniumyl substituents of the porphyrin ring system are electron deficient and may be electroreducible in the potential range −0.2 to −1.0 V, as has been demonstrated for other non-porphyrin compounds with *N*-methylpyridiniumyl groups.[18,19] Thus, in principle, a total of six electrons may be added to the TMpyP porphyrin moiety, two electrons to the π ring system and four to the *N*-methylpyridiniumyl groups. However, this has never been demonstrated since most previous studies of TMpyP free base and metalated derivatives have been carried out in aqueous media.

A recent report on the electrochemistry of (TMpyP)Ni(ClO$_4$)$_4$ shows a dimer–monomer equilibrium of this complex in *N*,*N*-dimethylformamide (DMF).[20] It was not clear if similar behavior would be observed for other metalated TMpyP derivatives in DMF, and this was investigated in the present work, which presents the first spectral and electrochemical characterization of [(TMpyP)Cu]$^{4+}$, [(TMpyP)Zn]$^{4+}$, and [(TMpyP)VO]$^{4+}$ in nonaqueous media. The structure of [(TMpyP)M]$^{4+}$, where M = Cu(II), Zn(II), or VO, is shown in Figure 1. As will be shown in this study, the three complexes exist as monomers in DMF and the formation of a phlorin does not occur upon electroreduction.

Experimental Section

Materials. Tetra-*n*-butylammonium perchlorate (TBAP) was purchased from Eastman Kodak Co., recrystallized from ethyl alcohol, and stored in a vacuum oven at 40 °C prior to use. The supporting electrolyte was 0.2 M TBAP for bulk electrolysis and spectroelectrochemical measurements and 0.1 M TBAP for polarographic and voltammetric measurements. *N*,*N*-Dimethylformamide (DMF) was vacuum distilled twice over 4-Å molecular sieves prior to use. DMF-d_7, purchased from Aldrich Co., was used as received.

Synthesis of *meso*-Tetrakis(1-methylpyridinium-4-yl)porphyrins. Free base [(TMpyP)H$_2$]$^{4+}$ was synthesized according to the procedure reported in ref 12, and [(TMpyP)Cu]$^{4+}$ and [(TMpyP)Zn]$^{4+}$ were prepared as described in ref 21 and 12, respectively. (TpyP)VO was also prepared as described in the literature[22] and was methylated by using the following procedure: A 1.8-g amount of (TpyP)VO and 2.94 g of methyl *p*-toluenesulfonate were refluxed in 250 mL of DMF for 4 h. The solvent was evaporated and the product dissolved in water and washed with CH$_2$Cl$_2$. The water was then evaporated and the solid product washed with hexane and acetone before drying under vacuum. The final product was recrystallized from DMF and washed with hexane. The obtained porphyrin was dried under vacuum and gave a yield of about 35% after recrystallization.

Instrumentation and Methods. UV–visible spectra of the initial complexes were recorded on an IBM 9430 spectrophotometer. ESR spectra were recorded on an IBM Model ER-100D electron spin resonance system. ESR measurements of the reduced complexes were taken after controlled-potential electrolysis under an inert atmosphere. The reduced

---

[1] (a) University of Houston. (b) Université de Dijon.

[2] Kalyanasundaram, K.; Gratzel, M. *Helv. Chim. Acta* **1980**, *63*, 478.

[3] Harriman, A.; Porter, G.; Richoux, M. C. *J. Chem. Soc., Faraday Trans. 2* **1981**, *77*, 833, 1939.

[4] Dougherty, T. J.; Kaufman, J. E.; Goldfarb, A.; Weishaupt, K. R.; Boyle, D.; Mittleman, A. *Cancer Res.* **1978**, *38*, 2628.

[5] Fiel, R. J.; Howard, J. C.; Mark, E. H.; Datta Gupta, N. *Nucleic Acids Res.* **1979**, *6*, 3093.

[6] Fiel, R. J.; Munson, B. R. *Nucleic Acids Res.* **1980**, *8*, 2835.

[7] Pasternack, R. F.; Gibbs, E. J.; Villafranca, J. J. *Biochemistry* **1983**, *22*, 2406.

[8] Pasternack, R. F.; Gibbs, E. J.; Gaudemer, A.; Antebi, A.; Bassner, S.; DePoy, L.; Turner, D. H.; Williams, A.; Laplace, F.; Lansarc, M. H.; Merienne, C.; Perree-Fauvet, M. *J. Am. Chem. Soc.* **1985**, *107*, 8179.

[9] Kano, K.; Miyake, T.; Uomoto, K.; Sato, T.; Ogawa, T.; Hashimito, S.; *Chem. Lett.* **1983**, 1867.

[10] Kano, K.; Nakajima, T.; Takei, M.; Hashimoto, S. *Bull. Chem. Soc. Jpn.* **1987**, *60*, 1281.

[11] Brookfield, R. L.; Ellul, H.; Harriman, A. *J. Photochem.* **1985**, *31*, 97.

[12] Pasternack, R. F.; Huber, P. R.; Boyd, P.; Engasse, G.; Francesconi, L.; Gibbs, E.; Fasella, P.; Venturo, G. C.; Hinds, L. d. C. *J. Am. Chem. Soc.* **1972**, *94*, 4511.

[13] Pasternack, R. G.; Spiro, E. G.; Teach, M. J. *Inorg. Nucl. Chem.* **1974**, *36*, 599.

[14] Hambright, P.; Neta, P.; Richoux, M.-C.; Abou-Gamra, Z.; Harriman, A. *J. Photochem.* **1987**, *36*, 255.

[15] Sazou, D.; Araullo, C.; Liu, Y. M.; Kadish, K. M. *Abstracts of Papers*, 194th ACS National Meeting of the American Chemical Society, New Orleans, LA; American Chemical Society: Washington, DC, 1987.

[16] Baral, S.; Hambright, P.; Neta, P. *J. Phys. Chem.* **1984**, *88*, 1594.

[17] Neta, P.; Richoux, M. C.; Harriman, A.; Baral, S.; Hambright, P. *J. Phys. Chem.* **1986**, *90*, 2462.

[18] Bird, C. L.; Kuhn, A. T. *Chem. Soc. Rev.* **1981**, *10*, 49.

[19] Bauer, R.; Nussbaumer, P.; Neumann-Spallart, M. *Z. Naturforsch.* **1988**, *43B*, 475.

[20] Kadish, K. M.; Sazou, D.; Liu, Y. M.; Saoiabi, A.; Ferhat, M.; Guilard, R. *Inorg. Chem.* **1988**, *27*, 686.

[21] Harriman, A.; Porter, G.; Walters, R. *J. Chem. Soc., Faraday Trans. 2* **1983**, *79*, 1335.

[22] Newton, C. M.; Davis, D. G. *J. Magn. Reson.* **1975**, *20*, 446.

0020-1669/89/1328-2528$01.50/0

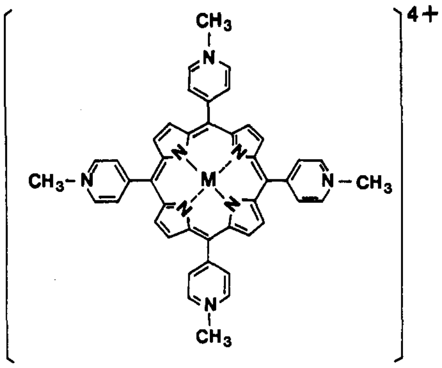

Figure 1. Simplified structures of [(TMpyP)M]$^{4+}$, where M = Cu(II), Zn(II), or VO.

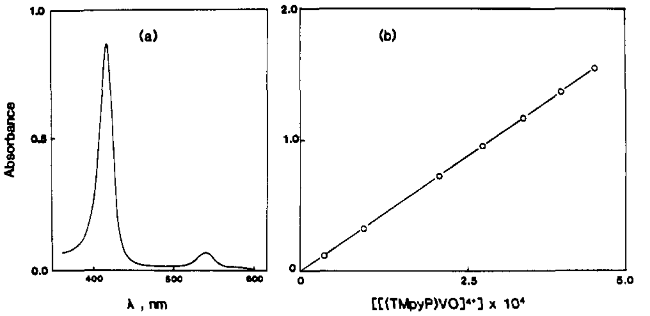

Figure 2. (a) Electronic absorption spectrum of 1.0 × 10^{-4} M [(TMpyP)VO]$^{4+}$ in DMF and (b) concentration dependence of [(TMpyP)VO]$^{4+}$ absorbance at 606 nm in DMF.

Table I. UV–Visible Spectral Data for [(TMpyP)M]$^{4+}$ and Its Reduction Products in DMF, 0.2 M TBAP at 23 °C

initial compd	electrode reacn	spectral product data: λ, nm (ε × 10^{-3})		
[(TMpyP)Cu]$^{4+}$	none[a]	424 (243)	544 (19.1)	582 (4.3)
	1st redn	484 (70.0)		832 (74.0)
	2nd redn	458 (53.0)	560 (8.0)	834 (38.7)
	3rd redn	448 (112)		834 (16.0)
[(TMpyP)VO]$^{4+}$	none[a]	439 (222)	564 (13.6)	606 (3.2)
	1st redn	489 (65.0)		855 (37.7)
	2nd redn	440 (46.0)	570 (7.0)	854 (25.8)
	3rd redn	440 (89.0)		854 (10.0)
[(TMpyP)Zn]$^{4+}$	none[a]	436 (288)	562 (23.2)	604 (7.0)
	1st redn	470 (73.7)		763 (76.1)
	2nd redn	452 (52.9)	570 (7.4)	755 (19.1)
	3rd redn	442 (80.0)		756 (10.0)

[a] Species before reduction.

samples were transferred to an ESR cell that was modified for use on a Schlenk line and then immediately frozen in liquid nitrogen. ^{1}H NMR spectra were taken on a QE-300 spectrometer with tetramethylsilane (TMS) as the internal standard.

Cyclic voltammetry, polarography, and bulk controlled-potential coulometry were carried out on a BAS 100 electrochemical analyzer or a Princeton Applied Research, EG&G, Model 174A/175 polarographic analyzer/potentiostat coupled with an Omnigraphic Houston 9002A X-Y recorder. The working and counter electrodes were platinum. A platinum minigrid electrode was used for the thin-layer spectroelectrochemical cell. The design of this cell is given in the literature.[23] Potentials were measured and reported versus a saturated calomel electrode (SCE), which was separated from the bulk solution by means of a fritted-glass disk junction. Thin-layer spectroelectrochemical measurements were made with an IBM EC 225 voltammetric analyzer, which was coupled with a Tracor Northern 6500 rapid-scan spectrometer/multichannel analyzer.

Results and Discussion

Electronic Absorption Spectra of [(TMpyP)M]$^{4+}$. Electronic absorption spectra of the three investigated compounds in DMF are summarized in Table I. Each complex has a Soret band in the range 424–439 nm and two visible bands in the range 544–606 nm. A representative spectrum of [(TMpyP)M]$^{4+}$ where M is VO is shown in Figure 2a.

Table II. ^{1}H NMR Chemical Shifts of [(TMpyP)Zn]$^{4+}$ at Different Concentrations in DMF-d_7[a]

porphyrin concn, M	types of protons: N-CH$_3$[b]	o-H[b]	m-H[b]	β-pyrrolic
7.0 × 10^{-4}	4.96 (s)	9.13 (d)	9.70 (d)	9.22 (s)
2.2 × 10^{-3}	4.96 (s)	9.12 (d)	9.69 (d)	9.22 (s)
6.4 × 10^{-3}	4.97 (s)	9.10 (d)	9.69 (d)	9.22 (s)

[a] s = singlet, d = doublet; shifts in ppm. [b] Protons of N-methylpyridiniumyl substituent.

Table III. Half-Wave Potentials (V vs SCE) and Peak Potential Differences between E_{pc} and E_{pa} (ΔE_p, mV) for Reduction of [(TMpyP)M]$^{4+}$ in DMF, 0.1 M TBAP at 23 °C (Scan Rate 0.1 V/s)

metal center	metal induction param[a]	$E_{1/2}$ (ΔE_p): I[b]	II[b]	III[b]
Zn^{II}	1.5	–0.65 (40)	–1.03 (35)	–1.14 (35)
Cu^{II}	1.9	–0.61 (35)	–0.89 (35)	–1.02 (35)
V^{II}O	3.0	–0.52 (33)	–0.85 (33)	–1.01 (35)

[a] See ref 34. [b] I–III correspond to the two-electron reductions illustrated in Figure 5.

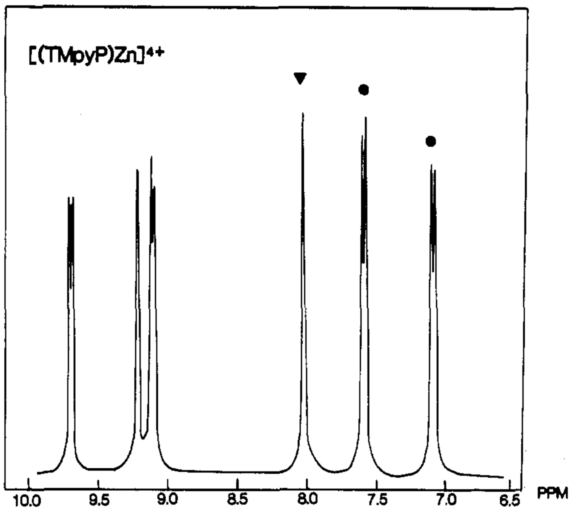

Figure 3. ^{1}H NMR spectrum of [(TMpyP)Zn]$^{4+}$ in deuterated DMF at T = 23 °C. The extra peaks are due to (▼) DMF and (●) the p-toluenesulfonate counterions. Similar spectra were obtained over the concentration range of 10^{-4} to 6 × 10^{-3} M (see Table II and text).

All three compounds follow Beer's law behavior in DMF between concentrations of 5 × 10^{-7} and 5 × 10^{-4} M, and this suggests that only one form of the porphyrin is present in solution. A Beer's law plot for [(TMpyP)VO]$^{4+}$ in the concentration range 2 × 10^{-5} to 5 × 10^{-4} M is shown in Figure 2b. The plot in this figure was constructed from absorptions at 606 nm. Similar plots were also obtained at 439 and 564 nm and also extrapolate to zero.

ESR and electrochemical data (see later sections) also suggest the presence of monomeric rather than dimeric [(TMpyP)M]$^{4+}$ in DMF. This is consistent with the fact that any coordinated DMF molecules would prohibit the closeness of approach required for the formation of dimers.[24,25]

^{1}H NMR Spectroscopy of Diamagnetic [(TMpyP)Zn]$^{4+}$. ^{1}H NMR chemical shifts of [(TMpyP)Zn]$^{4+}$ at different concentrations in deuterated DMF are summarized in Table II, and the ^{1}H NMR spectrum of this porphyrin at 2.2 × 10^{-3} M is illustrated in Figure 3. Unlike spectra of tetraphenylporphyrins,[26] the m-H

---

(23) Lin, X. Q.; Kadish, K. M. *Anal. Chem.* **1985**, *57*, 1498.

(24) Krishnamurthy, M.; Sutter, J. R.; Hambright, P. *J. Chem. Soc., Chem. Commun.* **1975**, 13.

(25) Corsini, A.; Herrmann, O. *Talanta* **1986**, *33*, 335.

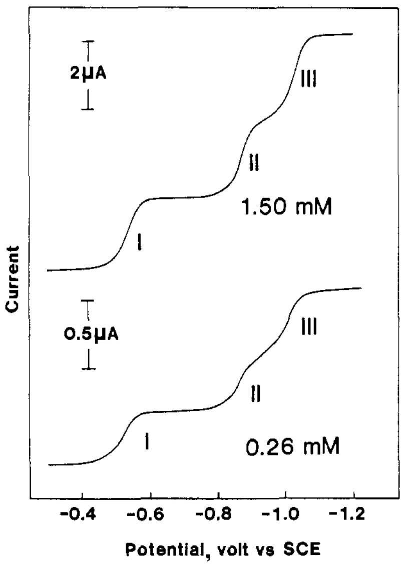

Figure 4. Dc polarograms illustrating the room-temperature reduction of $[(TMpyP)VO]^{4+}$ at two concentrations in DMF, 0.1 M TBAP.

peaks of the *N*-methylpyridiniumyl group are shifted downfield by 0.47 ppm from the β-H pyrollic peaks. Such a result can be attributed to the proximity of these protons to the positively charged *N*-methyl groups of the substituents. No variation in chemical shifts are observed with changes in porphyrin concentration (see Table II), which suggests the presence of only one form of the porphyrin in DMF, i.e., a monomer. In addition, the ^1H NMR spectra of $[(TMpyP)Zn]^{4+}$ over the concentration range shown in Table II are different from the reported spectra of $[(TMpyP)Ni]^{4+}$, which exists in a monomer–dimer equilibrium.[20]

Electroreduction of $[(TMpyP)M]^{4+}$. Figure 4 shows dc polarograms for the reduction of 1.50 and 0.26 mM $[(TMpyP)VO]^{4+}$ in DMF containing 0.1 M TBAP. The reductions occur at $E_{1/2}$ = −0.53, −0.87, and −1.02 V and are labeled as reactions I, II, and III, respectively. Each $E_{1/2}$ value is independent of the bulk concentration between 3×10^{-4} and 2.5×10^{-3} M. The limiting currents, which are equal for each of the reductions over this concentration range, are also directly proportional to the bulk concentration of the porphyrin and increase linearly with the square root of the mercury height. Wave analysis gives slopes that range between 30 and 35 mV, thus implying the overall diffusion-controlled addition of two electrons in each of the three electron-transfer steps.

Figure 5 illustrates cyclic voltammograms for the reduction of $[(TMpyP)VO]^{4+}$, $[(TMpyP)Cu]^{4+}$, and $[(TMpyP)Zn]^{4+}$ in DMF. All three voltammograms are qualitatively similar, and the half-wave potentials for reduction processes I, II, and III by cyclic voltammetry are listed in Table III. The peak currents for each reduction in Figure 5 increase linearly with the square root of scan rate and half-wave potentials for each process are independent of scan rate, thus indicating uncomplicated diffusion-controlled two-electron-transfer processes for the electroreduction at room temperature.

The results from thin-layer coulometric reduction of $[(TMpyP)VO]^{4+}$, $[(TMpyP)Zn]^{4+}$, and $[(TMpyP)Cu]^{4+}$ are consistent with the room-temperature cyclic voltammetric and polarographic data in that processes I, II, and III involve two electrons in each reduction step. A thin-layer controlled-potential electrolysis carried out at −1.2 V also shows the global addition of six electrons for the three complexes, and a coulometric value of two electrons is obtained by controlled-potential reduction of each compound at −0.7 V. However, bulk controlled-potential coulometry invariably gave less than two electrons transferred in the second and third reduction steps. This difference between the stepwise bulk electrolysis results, and electrochemical data from the other voltammetric techniques may be attributed either to an adsorption of the species electrogenerated after the first controlled-potential electrolysis[27] or to a protonation reaction,[28] which might occur only on the slower bulk electrolysis time scale.

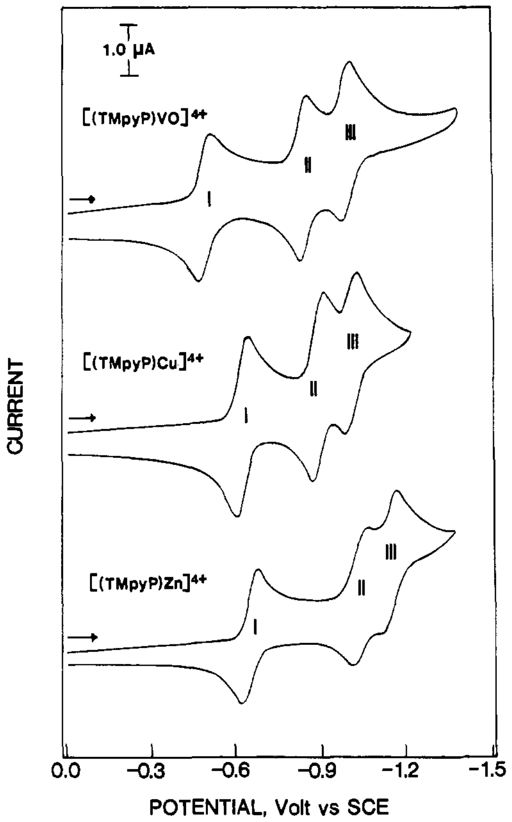

Figure 5. Cyclic voltammograms illustrating the room-temperature reduction of the $[(TMpyP)M]^{4+}$ complexes in DMF, 0.1 M TBAP (scan rate 0.1 V/s).

The electronic absorption spectrum of $[(TMpyP)VO]^{2+}$ obtained after controlled-potential reduction by two electrons is shown in Figure 6a, and thin-layer spectra of the species produced in processes II and III are illustrated in Figure 6b,c, respectively. A spectrum similar to the one illustrated in Figure 6a has been presented for the species generated after a two-electron reduction of $[(TMpyP)Al]^{5+}$. However, in this latter case, there is a single protonation at the meso position of the porphyrin.[16] This type of reaction does not occur for the investigated compounds in DMF, and the spectrum of the species generated after electrolysis of $[(TMpyP)VO]^{4+}$ at −0.70 V (see Figure 6a) is assigned as due to $[(TMpyP)VO]^{2+}$.

The spectrum obtained after controlled-potential reduction of $[(TMpyP)VO]^{2+}$ at −0.95 V (Figure 6b) is assigned to a four-electron-reduced product, (TMpyP)VO. A broad absorption band is centered at 570 nm and is close to the wavelength where one-electron-reduced methyl viologen type anions generally absorb[19] (between 600 and 610 nm). The UV–visible spectrum of the six-electron-reduced product, $[(TMpyP)VO]^{2-}$, has decreased absorption bands at 853 and 570 nm and a moderately strong band at 440 nm (see Figure 6c). Similar spectral changes are observed for $[(TMpyP)Cu]^{4+}$ and $[(TMpyP)Zn]^{4+}$, and these thin-layer spectroelectrochemical data are summarized in Table I along with those for $[(TMpyP)VO]^{4+}$.

Cyclic voltammograms of $[(TMpyP)Cu]^{4+}$ and $[(TMpyP)Zn]^{4+}$ at three temperatures are shown in Figure 7. A similar temperature-dependent voltammogram was also obtained for $[(TMpyP)VO]^{4+}$. As the temperature is decreased from 23 to −55 °C, the first reduction becomes irreversible while processes II and III remain unchanged. The low-temperature data suggests the occurrence of a chemical reaction following the first reduction

---

[26] Eaton, S. S.; Eaton, G. R. *J. Chem. Soc., Chem. Commun.* **1974**, 576.

[27] The Pt electrode was coated with a dark layer of porphyrin, indicating either strong adsorption or precipitation of the porphyrin.

[28] Lanese, J. G.; Wilson, G. S. *J. Electrochem. Soc.* **1972**, *119*, 1039.

Table IV. ESR Data for Copper and Vanadyl Complexes in DMF, 0.1 M TBAP at -100 °C[a]

compd	$g_\parallel$	$g_\perp$	${}^{M}A_\parallel \times 10^{4\,b}$	${}^{M}A_\perp \times 10^4$	${}^{N}A_\parallel \times 10^4$	${}^{N}A_\perp \times 10^4$
$[(\text{TMpyP})\text{Cu}]^{4+\,c}$	2.170	2.056	182	31	13	15
$[(\text{TMpyP})\text{Cu}]^{4+}$	2.192	2.062	194	27	14	13
$[(\text{TMpyP})\text{Cu}]^{2+\,d}$	2.174	2.052	214	32	16	16
$(\text{TMpyP})\text{Cu}^{e}$	2.156	2.043	219	33	16	16
$[(\text{TMpyP})\text{Cu}]^{2-\,f}$	2.159	2.051	231	31	17	14
$[(\text{TMpyP})\text{VO}]^{4+}$	1.985	2.010	159	54		
$[(\text{TMpyP})\text{VO}]^{2+\,d}$	1.974	2.001	177	56		
$(\text{TMpyP})\text{VO}^{e}$	1.972	2.013	182	59		
$[(\text{TMpyP})\text{VO}^{2-\,f}$	1.968	2.014	184	60		

[a] All coupling constants A are expressed in units of cm^{-1}. [b] Where M = Cu(II) or VO. Error limits are ±0.002 for g values and ±5% for A values. [c] Solvent = pyridine. [d] After electrolysis at -0.70 V. [e] After electrolysis at -0.95 V. [f] After electrolysis at -1.20 V.

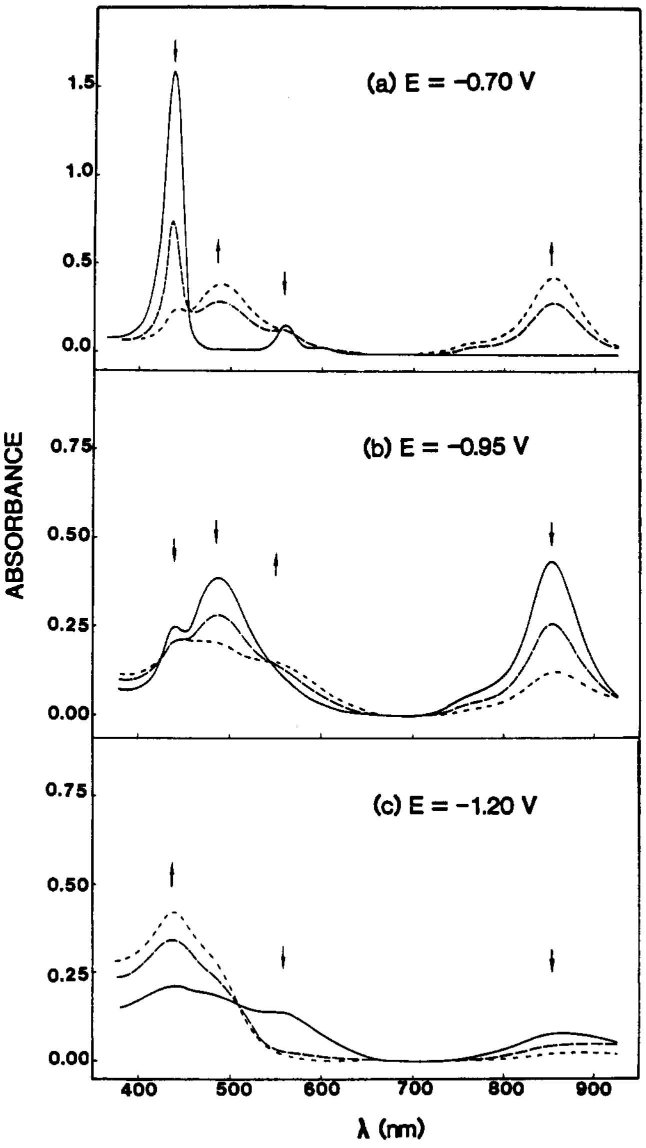

Figure 6. (a) Time-resolved electronic absorption spectra obtained during thin-layer controlled-potential electrolysis of 1.75×10^{-4} M $[(\text{TMpyP})\text{VO}]^{4+}$ in DMF, 0.2 M TBAP at (a) -0.70 V, (b) -0.95 V, and (c) -1.20 V.

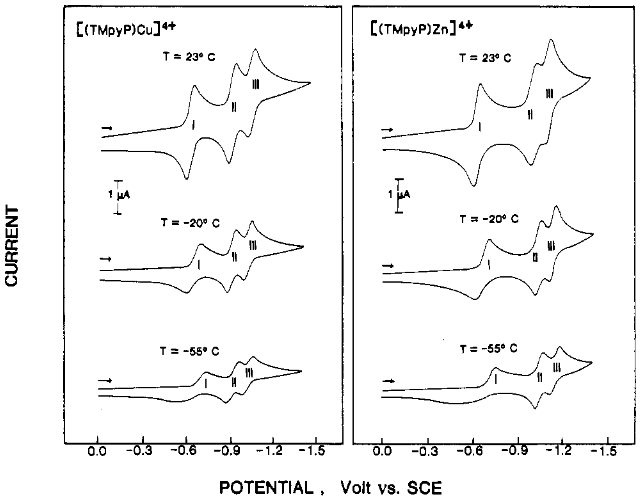

Figure 7. Cyclic voltammograms illustrating the reduction of $[(\text{TMpyP})\text{Cu}]^{4+}$ and $[(\text{TMpyP})\text{Zn}]^{4+}$ in DMF, 0.1 M TBAP at variable temperature (scan rate 0.1 V/s).

process, but the low-temperature spectra of the products generated by processes I (as well as those of II and III) were almost indistinguishable from the room-temperature spectra that are shown in Figure 6 for $[(\text{TMpyP})\text{VO}]^{4+}$.

A room-temperature dimerization of $[(\text{TMpyP})\text{M}]^{(n-1)+}$, where M = Al(III) ($n$ = 5) or Zn(II) (n = 4), has been invoked by pulse-radiolysis studies of $[(\text{TMpyP})\text{M}]^{n+}$,[16] and a dimerization of the $[(\text{TMpyP})\text{M}]^{2+}$ complexes could be invoked in this present study to explain the irreversibility of process I at low temperature. However, no spectral evidence was obtained that could support the formation of a dimer. In addition, processes II and III should be affected by a dimerization of the complex after the first reduction and no changes in the current-voltage curves consistent with this assignment were obtained.

A more likely explanation for the temperature dependence of the voltammograms in Figure 7 is that the TMpyP complexes undergo a change in coordination after the first two-electron reduction. It is known that the first reductions of (P)VO, where P = TpyP, TPPS and TPP, are accompanied by a loss of solvent ligand,[29] and a similar loss of solvent is postulated to occur after reduction of $[(\text{TMpyP})\text{VO}]^{4+}$, $[(\text{TMpyP})\text{Zn}]^{4+}$, and $[(\text{TMpyP})\text{Cu}]^{4+}$. Under these conditions the overall reduction mechanism for process I would be as follows, where M = Cu(II), Zn(II) or VO:

$$[(\text{TMpyP})\text{M}(\text{DMF})]^{4+} \xrightleftharpoons{+2e^-} [(\text{TMpyP})\text{M}(\text{DMF})]^{2+} \xrightleftharpoons{\text{fast}} [(\text{TMpyP})\text{M}]^{2+} + \text{DMF} \quad (1)$$

At -55 °C, the reassociation rate of DMF with $[(\text{TMpyP})\text{M}]^{2+}$ would be slowed down, thus preventing a reformation of $[(\text{TMpyP})\text{M}(\text{DMF})]^{2+}$ before reoxidation to give the initial $[(\text{TMpyP})\text{M}(\text{DMF})]^{4+}$. The unsolvated $[(\text{TMpyP})\text{M}]^{2+}$ should be harder to oxidize than solvated $[(\text{TMpyP})\text{M}(\text{DMF})]^{2+}$, and if the ligation rate of the reduced complex is slow prior to reoxidation, an apparent irreversibility (an electrochemical CE type mechanism) could be observed in the reoxidation. This irreversibly would not occur at 23 °C, where the rate of DMF association with $[(\text{TMpyP})\text{M}]^{2+}$ would be considerably higher.

ESR Spectroscopy of $[(\text{TMpyP})\text{Cu}]^{4+}$ and $[(\text{TMpyP})\text{VO}]^{4+}$ before and after Electroreduction. ESR spectra of $[(\text{TMpyP})\text{Cu}]^{4+}$ were recorded at both room and low temperature. An isotropic spectrum is obtained at 23 °C, and the spectrum is axially sym-

---

(29) Kadish, K. M.; Sazou, D.; Araullo, C.; Liu, Y. M.; Saoiabi, A.; Ferhat, M.; Guilard, R. *Inorg. Chem.* **1988**, *27*, 2313.

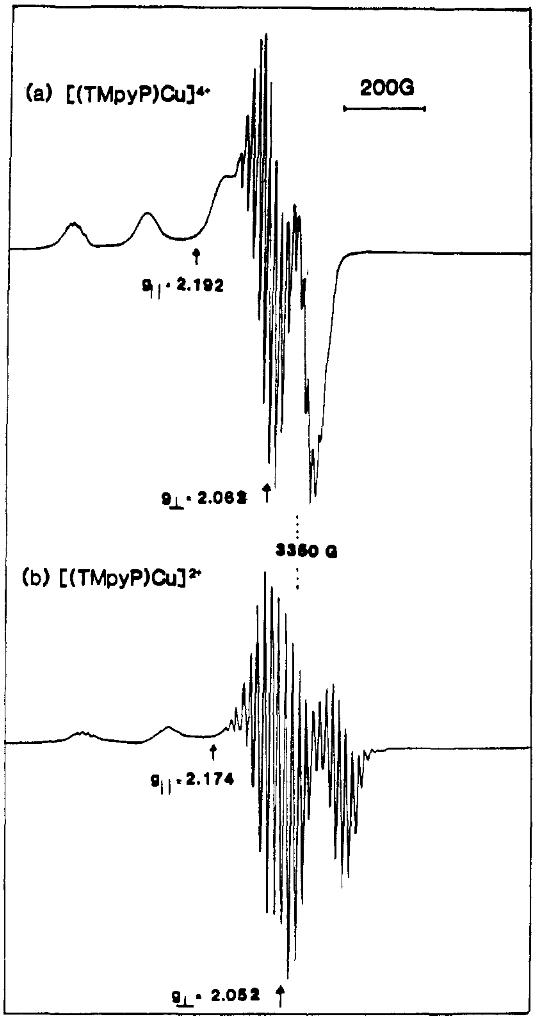

Figure 8. ESR spectra of $[(TMpyP)Cu]^{4+}$ and electrogenerated $[(TMpyP)Cu]^{2+}$ in DMF, 0.2 M TBAP at −100 °C.

metric at −100 °C. Spin-Hamiltonian parameters calculated for $[(TMpyP)Cu]^{4+}$ in DMF and py are similar to values for monomeric $[(TPPS)Cu]^{4-}$ in the same solvent,[30] and are listed in Table IV. A change in the concentration of $[(TMpyP)Cu]^{4+}$ from 1×10^{-4} to 5×10^{-2} M did not influence the ESR parameters at either high or low temperatures, thus indicating an absence of aggregation for this Cu(II) complex.

ESR spectra of $[(TMpyP)Cu]^{4+}$ and electrogenerated $[(TMpyP)Cu]^{2+}$ in DMF at −100 °C are shown in Figure 8. As expected, the ESR spectrum of $[(TMpyP)Cu]^{2+}$ is almost identical with the spectra of (TMpyP)Cu and $[(TMpyP)Cu]^{2-}$ that are generated after the second and third two-electron reductions at −0.95 and −1.20 V, respectively (see Table IV). No ESR signals were observed at the half-field region ($g \sim 4$) in these spectra.

Measured $g_{\parallel}$ and $g_{\perp}$ values for the reduced Cu(II) and VO porphyrins are relatively smaller than for the unreduced complexes. However, the ${}^{Cu}A_{\parallel}$ value is increased for the reduced porphyrins compared to corresponding values for the neutral forms of the complex (see Figure 8 and Table IV). This is not surprising since the added two electrons would alter the charge distribution on the macrocycle and consequently the electronic structure of the metal center.

ESR spectra obtained after the two-, four-, and six-electron reductions of $[(TMpyP)VO]^{4+}$ are similar, and this spectral data is listed in Table IV. The similarities in ESR spectral parameters for the neutral and reduced forms of both the Cu and VO porphyrins and the absence of a signal in the $g = 4$ region for the Cu(II) complexes strongly suggest that these complexes do not exist as axial dimers.[31] The ESR data also suggests the absence of metal-centered reductions of Cu(II) or VO occurs under the present experimental conditions.

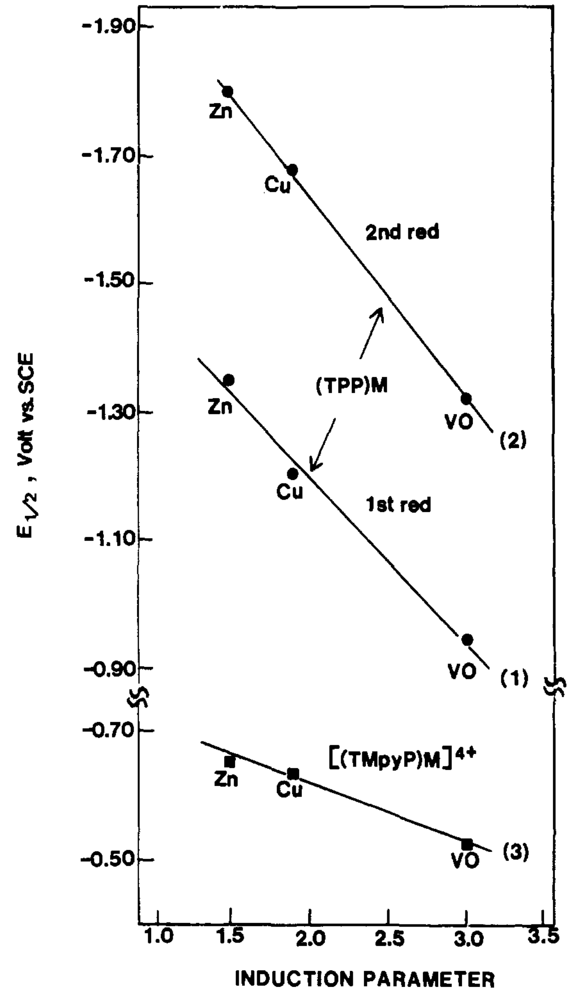

Figure 9. Plots of $E_{1/2}$ vs induction parameter of the metal (see ref 34) for the porphyrin π-ring-centered reductions of (●) (TPP)M and (■) $[(TMpyP)M]^{4+}$ in DMF, 0.1 M TBAP. The former compounds are reduced in two one-electron-transfer steps while the latter reaction occurs via a single two-electron-transfer process.

Site of Electron Transfer. The voltammetric, spectroelectrochemical, and ESR results for the reduction of $[(TMpyP)M]^{4+}$, where M = Cu(II), Zn(II), and VO are all self-consistent and suggest the following sequence of electron-transfer steps, where L = DMF and n = 1 or 2.

$$[(TMpyP)M(L)_n]^{4+} + 2e^- \rightleftarrows [(TMpyP)M]^{2+} + nL \quad (2)$$

$$[(TMpyP)M]^{2+} + 2e^- \rightleftarrows (TMpyP)M \quad (3)$$

$$(TMpyP)M + 2e^- \rightleftarrows [(TMpyP)M]^{2-} \quad (4)$$

Reactions 3 and 4 have not been previously reported, but the two-electron reduction described in eq 2 is consistent with data in the literature[32,33] for electroreduction of both $[(TMpyP)H_2]^{4+}$ and $[(TMpyP)Mn]^{5+}$. Hambright and Williams[20] reported the simultaneous addition of two electrons for the electroreduction of $[(TMpyP)H_2]^{4+}$ in DMF, and the same authors also report that a simultaneous two-electron-reduction process occurs for $[(TMpyP)Mn]^{5+}$ subsequent to the Mn(III)/Mn(II) electron transfer in the same solvent. $[(TMpyP)H_2]^{4+}$ is also reduced by

---

(30) DeBolfo, J. A.; Smith, T. D.; Boas, J. F.; Pilbrow, J. R. *J. Chem. Soc., Dalton Trans.* **1975**, 1523.

(31) Subramanian, J. In *Porphyrins and Metalloporphyrins*; Smith, K. M., Ed.; Elsevier: Amsterdam, 1975; Chapter 13.

(32) Hambright, P.; Williams, R. F. In *Porphyrin Chemistry Advances*; Longo, F. R., Ed.; Ann Arbor Sciences: Ann Arbor, MI, 1979; pp 284–292.

(33) Neri, B.; Wilson, G. *Anal. Chem.* **1972**, *44*, 1002.

a single two-electron-transfer step in H_2O, but in this case, the electrode reaction is irreversible and involves the formation of a hydroporphyrin.[33]

The formation of porphyrin π anion radicals and dianions in the reduction of (P)M, where P = OEP, occurs at $E_{1/2}$ values that can be correlated to the electronegativity of the metal ion.[34] Plots of $E_{1/2}$ vs an electronegativity parameter for the reduction of OEP complexes are linear,[34] and this is also the case for the reduction of TPP and TMpyP metal complexes, as shown in Figure 9. As seen in this figure, a similar qualitative trend is observed by using the $E_{1/2}$ of process I for [(TMpyP)M]$^{4+}$ reduction. This two-electron reduction of [(TMpyP)Cu]$^{4+}$, [(TMpyP)Zn]$^{4+}$, and [(TMpyP)VO]$^{4+}$ occurs at the porphyrin π ring and generates [(TMpyP)M]$^{2+}$ as shown in eq 2.

Figure 9 also shows plots of $E_{1/2}$ for the first and second reductions of the TPP complexes as described in eq 5 and 6. As

$$\text{(TPP)M} + e^- \rightleftarrows [\text{(TPP)M}]^- \tag{5}$$

$$[\text{(TPP)M}]^- + e^- \rightleftarrows [\text{(TPP)M}]^{2-} \tag{6}$$

shown in this figure, all three plots are linear and the reduction of [(TMpyP)M]$^{4+}$ occurs at $E_{1/2}$ values that are shifted positively by as much as 420–1150 mV relative to those of the corresponding (TPP)M species. In addition, the difference in potential between $E_{1/2}$ for the two successive one-electron additions to (TPP)M ranges from ~400 to ~500 mV while a value of 0 mV is obtained for the two-electron reduction of [(TMpyP)M]$^{4+}$. Interestingly, the slope of the plots for the one-electron-transfer reactions of (TPP)M are higher than the slope for the corresponding plot involving [(TMpyP)M]$^{4+}$, which undergoes a simultaneous addition of two electrons.

The values of $E_{1/2}$ for processes II and III are given in Table III and do not show a linear correlation with the induction parameter of the central metal ion. In addition, processes II and III are insensitive to changes in temperature and occur in a similar potential range for all monomeric TMpyP complexes.[32,35] They are therefore assigned to an overall four-electron reduction of the four *N*-methylpyridiniumyl substituents. A reduction of the *N*-methylpyridiniumyl substituents was not observed for the case of (TMpyP)Ni$(ClO_4)_4$.[20] However, this porphyrin exists in a dimer–monomer equilibrium and the dimerization of the compound may shift the *N*-methylpyridiniumyl reductions beyond the solvent limit. Finally, the similar electrochemical behavior for processes II and III at high and low temperatures is consistent with a lack of solvent binding to the oxidized or reduced forms of the complex.

Conclusion. A comparison of the electrochemistry for (TPP)M and [(TMpyP)M]$^{4+}$, where M = Cu(II), Zn(II) and VO, shows that the presence of the positively charged *N*-methylpyridiniumyl substituents shift the porphyrin ring reduction potential positively by as much as 420–1150 mV with respect to a (TPP)M complex with the same metal. In addition, two electrons are simultaneously added to the porphyrin ring of the [(TMpyP)M]$^{4+}$ complexes while (TPP)M is similar to other (P)M complexes in that the electroreduction at the porphyrin π ring system occurs in two well-separated one-electron-transfer steps. Finally, a reduction of the *N*-methylpyridiniumyl groups occurs in the potential range −0.8 V to −1.1 V, which results in a total of six electrons added to these complexes.

Acknowledgment. The support of the National Science Foundation (Grants No. CHE-8515411 and INT-8413696) is gratefully acknowledged. We also acknowledge the help of Y. M. Liu in performing several preliminary experiments on [(TMpyP)VO]$^{4+}$.

Registry No. [(TMpyP)Cu]$^{4+}$, 48242-70-2; [(TMpyP)Cu]$^{2+}$, 119851-11-5; [(TMpyP)Cu], 119851-12-6; [(TMpyP)Cu]$^{2-}$, 119851-13-7; [(TMpyP)VO]$^{4+}$, 106049-21-2; [(TMpyP)VO]$^{2+}$, 119851-14-8; [(TMpyP)VO], 119851-15-9; [(TMpyP)VO]$^{2-}$, 119851-16-0; [(TMpyP)Zn]$^{4+}$, 40603-58-5; [(TMpyP)Zn]$^{2+}$, 119851-17-1; [(TMpyP)Zn], 119851-18-2; [(TMpyP)Zn]$^{2-}$, 119851-19-3; [(TMpyP)Co]$^{4+}$, 79346-65-9; [(TMpyP)Fe]$^{5+}$, 60489-13-6; DMF, 68-12-2.

---

[34] Fuhrhop, J.-H.; Kadish, K. M.; Davis, D. G. *J. Am. Chem. Soc.* **1973**, *95*, 5140.

[35] Unpublished results on [(TMpyP)Co]$^{4+}$ and [(TMpyP)Fe]$^{5+}$ also show that each compound undergoes two two-electron-transfer processes in the potential range −0.9 to −1.1 V.